Effect of polyaniline (PANI) on efficiency enhancement of dye-sensitized solar cells fabricated with poly(ethylene oxide)-based gel polymer electrolytes

J. M. K. W. Kumari, G. K. R. Senadeera, A. M. J. S. Weerasinghe, C. A. Thotawatthage & M. A. K. L. Dissanayake

Journal of Solid State Electrochemistry
Current Research and Development in Science and Technology

ISSN 1432-8488

J Solid State Electrochem
DOI 10.1007/s10008-020-04841-6

Springer

Journal of Solid State Electrochemistry
https://doi.org/10.1007/s10008-020-04841-6

ORIGINAL PAPER

Effect of polyaniline (PANI) on efficiency enhancement of dye-sensitized solar cells fabricated with poly(ethylene oxide)-based gel polymer electrolytes

J. M. K. W. Kumari[1,2] · G. K. R. Senadeera[1,3] · A. M. J. S. Weerasinghe[1] · C. A. Thotawatthage[1] · M. A. K. L. Dissanayake[1]

Received: 29 June 2020 / Revised: 3 October 2020 / Accepted: 7 October 2020

Abstract

Ionically conducting gel polymer electrolytes can be used effectively to improve the problems associated with liquid electrolytes in dye-sensitized solar cells (DSSCs) and in particular to reduce their electrode degradation. In this work, gel polymer electrolytes containing poly(ethylene oxide) (PEO), LiI, and I_2 were used as the redox electrolyte and conducting polymer; polyaniline (PANI) as an additive was introduced to the PEO-based electrolytes. The effect of incorporating PANI into the PEO-based gel electrolyte on iodide ion conductivity and solar cell performance was studied. The gel polymer electrolyte without PANI showed a conductivity of 1.23×10^{-3} S cm^{-1} at room temperature, while the electrolyte incorporating 1.5 wt% PANI showed an enhancement in conductivity increasing its value up to 1.87×10^{-3} S cm^{-1}. While the DSSCs fabricated without PANI in the electrolyte showed 5.00% efficiency, the DSSCs fabricated with 1.5 wt% PANI-incorporated polymer electrolyte showed 6.56% efficiency under the same illumination of 100 mW cm^{-2}(AM 1.5) simulated sunlight. Ionic conductivity and FTIR results suggest that the increase in electrolyte conductivity and the enhancement of DSSC performance appear to be due to the combined result of the plasticizing effect on decreasing the crystallinity of the PEO polymer and the improved ionic dissociation due to "trapping" and immobilizing the Li^+ cations in the polymer matrix by PANI, creating more iodide (I^-) ions in the redox medium.

Keywords Dye-sensitized solar cell · PEO-based gel electrolyte · Cation trapping · PANI incorporation

Highlights
- Gel polymer electrolytes containing poly(ethylene oxide), LiI, and I_2 were studied.
- Electrolyte conductivity increased substantially due to addition of PANI conducting polymer.
- The dye solar cell efficiency increased from 5.00 to 6.56% due to PANI addition.
- Conductivity and FTIR data suggest that PANI acts as a plasticizer.
- PANI also appears to "trap" and immobilize the Li^+ cations promoting ionic dissociation.

✉ M. A. K. L. Dissanayake
makldis@yahoo.com

[1] National Institute of Fundamental Studies, Kandy 2000, Sri Lanka

[2] Postgraduate Institute of Science, University of Peradeniya, Peradeniya 20400, Sri Lanka

[3] Department of Physics, The Open University of Sri Lanka, Nawala, Nugegoda 10250, Sri Lanka

Introduction

After the first report by O'Regan and Gratzel in 1991, dye-sensitized solar cells (DSSCs) have been extensively studied and developed due to their lower fabrication cost, relatively higher efficiencies, and simple fabrication technology. A DSSC mainly consists of a dye-adsorbed semiconductor photoanode, a counter electrode, and a redox electrolyte, in which the electrolyte plays an important role as the charge transport medium. Majority of the DSSCs studied so far generally employ a liquid electrolyte–based I^-/I_3^- redox couple and have impressive energy conversion efficiencies of the order of 8–12%. However, the lack of long-term stability due to the leakage of the liquids, electrode corrosion, and photodecomposition of the dye in the solvent medium due to the usage of volatile liquids are some of the major drawbacks preventing large-scale long-term practical applications of liquid electrolyte–based DSSCs [1, 2].

Published online: 21 October 2020

During the past decade, researches on DSSCs based on aqueous electrolytes have emerged due to the stability issues in non-aqueous electrolyte–based cells. B. O'Regan et al. in 2010 [3] have studied the one sun current–voltage (*I-V*) performance of DSSCs fabricated with the TG6 dye and electrolytes with different water contents. They have reported that, with up to 40% of water in the electrolyte, the efficiencies remained around 5.5%. In the last few years, the research community has started using water as a solvent, and a substantial amount of research articles have been published on this topic [4–8]. By means of DSSCs fabricated with water-based electrolytes, reduced costs, non-flammability, reduced volatility, and improved environmental compatibility can be easily achieved. Along with these developments, an increasing number of novel electrodes, dyes, and electrolyte components are continuously being proposed, which are highly challenging from the materials science viewpoint [4]. The efficiency recorded up to now for a 100% water-based DSSC is 5.97%, as obtained by Lin et al. in 2015, in combination with a metal-free organic dye (EO3) and TEMPO/iodide electrolyte [8]. However, most of the studies in this research area have shown energy conversion efficiencies below 3%.

Multifunctional energy devices with various energy forms in different operation modes are under current research focus toward the new-generation smart and self-powered electronics. Recent progress has been made in developing integrated/joint multifunctional energy devices, with a focus on electrochromic batteries/supercapacitors, and solar cells–powered batteries/supercapacitors [9]. A dye-sensitized solar module (DSSM) and a high-voltage all-solid-state electrochemical double-layer capacitor (EDLC) have, for the first time, demonstrated in 2008 in a compact harvesting-storage (HS) device [10].

Transparent DSSCs can be coupled within a building's architecture to provide day lighting and electrical power simultaneously. Enhancing the efficiency of transparent dye-sensitized solar cells using concentrated light has been reported by Selvaraj et al. [11]. In their work, the relationship between the transparency and performance of DSSCs has been studied by changing the TiO_2 electrode thickness. The 10-μm-thick device has shown a power conversion efficiency of 5.93% with 37% transparency in the visible range. Current research activities also deal with smart architectural glazing windows and panels in buildings. In this context, highly performing technologies, such as semitransparent photovoltaics and novel photoelectrochromic devices, are expected to reach the final stage of development, leading to multifunctional, smart glazing windows [12].

In the case of dye-sensitized solar cells, although fully solid-state electrolytes improve the durability because of their good chemical and thermal stability in extreme environmental conditions, the large charge resistance at electrolyte/electrode interfaces reduces charge extraction and overall solar cell performance [13]. One of the solutions to overcome this problem is to introduce quasi-solid or gel electrolytes having fast charge transfer processes and low interfacial resistance compared to solid electrolyte–based cells [14].

The polymers used in gel polymer electrolytes usually contain ether oxygen atoms for supporting dissolution of the ionic salt. In this context, high molecular weight poly(ethylene oxide) (PEO) polymer has been extensively studied for the preparation of gel polymer electrolytes because of its ability to dissolve a variety of inorganic salts (lithium, magnesium salts, etc.) leading to polymer electrolytes with significantly high ionic conductivity. In these PEO-based polymer gel electrolytes, ether oxygen atoms facilitate the cation transport mechanism called the hopping mechanism and the anion transport occurs by diffusion [15, 16]. The presence of the ionic salt also reduces the crystallinity of the PEO matrix and increases the amorphous phase content which affects favorably for ionic transport. Even though there are few reports on the incorporation of electronically conducting polymers such as polyaniline or polypyrrole to the PEO-based electrolytes resulting enhancement in ionic conductivity of the electrolyte, detailed studies and mechanisms have not been discussed extensively [17, 18]. Therefore, in this work, a detailed investigation was carried out in order to understand the effect of incorporation of PANI in the PEO-based electrolytes on the ionic transport and efficiency enhancement in DSSCs.

Materials and methods

PANI-incorporated gel polymer electrolytes were prepared by mixing 0.264 g of PEO (Mw = 400,000, Sigma-Aldrich), 0.1 g of LiI (Sigma-Aldrich), 0.019 g of I_2 (Sigma-Aldrich), 1.5 ml of acetonitrile (anhydrous, Sigma-Aldrich), and different amounts of PANI emeraldine salt (average Mw. > 15,000, Sigma-Aldrich). PANI amounts were selected as 0.5, 1.0, 1.5, 2.0, and 2.5 wt% of PEO weight and for the comparison, a control electrolyte was prepared without adding PANI (0 wt% PANI). All weighted chemicals were thoroughly mixed and continuously stirred using a magnetic stirrer for about 12 h.

Double-layered TiO_2 photoanodes were prepared as reported in the literature [9], using the spin coat method and the doctor-blade method. For this, P90 TiO_2 powder (Evonik) and P25 TiO_2 powder (Degussa) were used and pastes prepared from these TiO_2 powders were deposited on fluorine-doped tin oxide (FTO) (8 Ω/sq, Solaronix) substrates layer after layer and sintered at 450 °C for 45 min after each layer. The sintered double-layer TiO_2 photoanodes were dipped in Ruthenium N719 (Solaronix) dye solution for 24 h. After dye adsorption, DSSCs were fabricated by sandwiching the aforementioned gel polymer electrolyte with dye-attached photoanode and Pt plated counter electrode for each electrolyte composition, keeping the thickness of the TiO_2

photoanode the same. For this, the gel electrolyte was kept on the dye-sensitized TiO_2 photoanode covering an area of 0.5 cm × 0.5 cm and the Pt counter electrode was kept over this to make the sandwich solar cell structure and the cell is then exposed to simulated sunlight. Subsequently, the two electrodes were gently pressed together to make the gel electrolyte penetrate into the nano-porous TiO_2 electrode surface until the photocurrent reached a maximum. By this method, we ensured that the electrolyte penetrated sufficiently into the photoanode surface.

Photovoltaic measurements of the DSSCs with an active cell area of 0.25 cm^2 were carried out by measuring the photocurrent-voltage (*J-V*) characteristics under the illumination of 100 mW cm^{-2} (AM 1.5) simulated sunlight using a computer-controlled measuring system coupled to a Keithley 2000 multimeter and a potentiostat/galvanostat HA-301. The efficiency of cells with a particular electrolyte composition has been measured at least five times to check the reproducibility. Electrochemical impedance spectroscopy (EIS) measurements were carried out on the DSSCs using a Metrohm Autolab potentiostat/galvanostat PGSTAT 128N with FRA 32 M frequency response analyzer (FRA) in the frequency range from 0.01 Hz to 1 MHz. These measurements were taken under the illumination of 100 mW cm^{-2} using the same solar simulator that was used for *J-V* measurements.

Electrolyte samples were characterized by Fourier transform infrared spectroscopy (ATR-FTIR, Bruker Alpha) to analyze the functional groups. The surface morphology of the prepared gel electrolytes without and with PANI was examined using scanning electron microscopy (SEM, Zeiss). Temperature dependence of the ionic conductivity of the gel polymer electrolyte samples was determined by the AC complex impedance method using a computer-controlled Autolab (PGSTAT 128N) impedance analyzer. For these measurements, the electrolyte sample was sandwiched between two stainless steel electrodes and placed inside a Teflon sample holder. The temperature of the sample was varied from about 25 to 65 °C with 5 °C intervals. For all the compositions studied, the ionic conductivity at each temperature was taken from the corresponding impedance plots.

Results and discussion

Photocurrent-voltage (J-V) analysis

The solar cell parameters obtained from photocurrent density-voltage (J-V) measurements on the DSSCs fabricated with gel polymer electrolytes containing different amounts of PANI are summarized in Table 1. It is clearly seen that the DSSCs fabricated with 1.5 wt% PANI-added electrolyte give the highest short circuit current density (J_{sc}) and highest power conversion efficiency. Figure 1 shows the J-V curves of the best DSSC fabricated using polymer electrolyte with the addition of 1.5 wt% PANI along with the control DSSC using the electrolyte without PANI.

Table 1 Photovoltaic parameters of the DSSCs with different amounts of PANI

Added PANI wt%	J_{sc} (mA cm^{-2})	V_{oc} (mV)	FF %	Efficiency %
0.0	11.76	698.0	60.86	5.00
0.5	13.81	652.8	60.97	5.50
1.0	14.35	651.5	64.51	6.03
1.5	16.23	630.2	64.13	6.56
2.0	16.17	617.2	64.15	6.31
2.5	16.02	611.8	64.34	5.94
5.0	11.40	601.7	56.09	3.85

The best DSSC fabricated without PANI in the PEO-based electrolyte showed 5.00% efficiency and the addition of 1.5 wt% PANI to the electrolyte has enhanced the efficiency to 6.56%. This is an impressive efficiency enhancement of 31% compared to the control DSSC made without PANI in the electrolyte. The enhancement in the short circuit current density due to the addition of PANI is a remarkable 38%. According to Table 1, the power conversion efficiency and J_{sc} gradually increase when the content of PANI in the electrolyte increases up to 1.5 wt%. However, when the amount of PANI exceeds 1.5 wt%, the efficiency and also the J_{sc} start to decrease.

In the PEO-based gel polymer electrolyte, the total ionic conductivity is due to the contributions from both Li^+ cations and I^- anions. As the short circuit photocurrent density in a DSSC with iodide/tri-iodide (I^-/I_3^-) redox couple is determined largely by the iodide ion (I^-) conductivity, the enhancement in the J_{sc} of the DSSCs made with the polymer

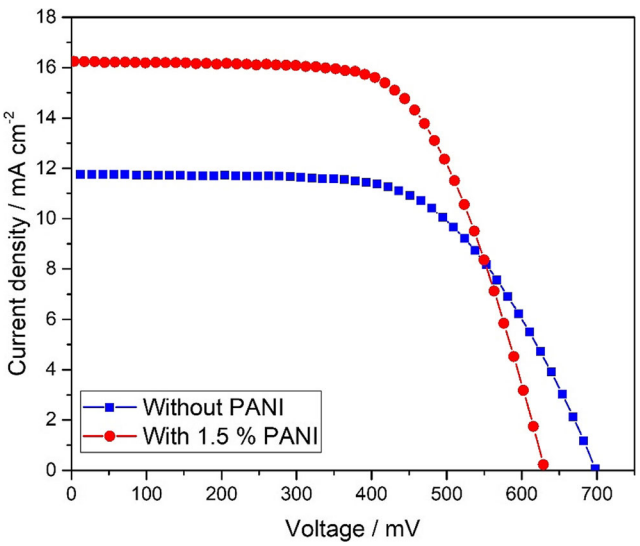

Fig. 1 Short circuit photocurrent density vs voltage curves of the DSSCs fabricated with PEO/LiI/I_2 and PEO/LiI/I_2/1.5 wt% PANI gel electrolytes

electrolyte having PANI used in the present work should be due to the increase in the number of iodide (I^-) anions or/and their mobility. Therefore, it is quite likely that the addition of PANI to the PEO-based electrolyte gives rise to two effects: (a) It increases the number of mobile iodide (I^-) ions in the electrolyte evidently by improved ionic dissociation due to the "*cation trapping effect*" and (b) at the same time, due to the plasticizing effect, PANI improves the anionic mobility in the electrolyte by increasing the amorphous phase content of the PEO electrolyte [19, 20]. The experimental data from the ionic conductivity measurements and FTIR spectroscopic measurements, described in detail in the subsequent sections, appear to support these possibilities.

EIS analysis

The charge transfer ability of the conducting gel electrolytes can be confirmed by the Nyquist plot obtained from EIS measurements of the DSSCs, as shown in Fig. 2. In the Nyquist plot, the first semicircle can be attributed to the electrochemical reaction resistance ($R1_{CT}$) at the Pt counter electrode in the high-frequency region. The middle semicircle indicates the charge transfer resistance ($R2_{CT}$) at the TiO_2/electrolyte interface in the mid-frequency region, while the third one is related to the diffusion of ions in electrolyte ($R3_{CT}$) [21].

Nyquist plots in Fig. 2 illustrate that all the charge transfer resistances for the cells made with 1.5 wt% PANI-added electrolyte are lower than those for the cells made with the electrolyte without PANI. By using a suitable equivalent circuit for the DSSC, values of interfacial resistances were estimated and are tabulated in Table 2. As can be seen from this table, $R3_{CT}$ value which corresponds to the diffusion of ions in the electrolyte medium is lower in the DSSC made with 1.5% wt% PANI-added electrolyte. This suggests that the I^-/I_3^- ions

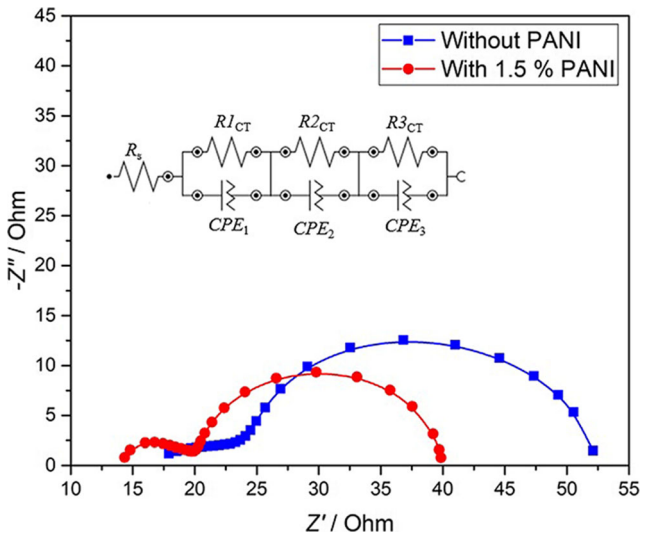

Fig. 2 Nyquist EIS plots of the DSSCs fabricated without PANI and with 1.5 wt% PANI in the gel polymer electrolyte

Table 2 Charge transfer resistances and electron lifetimes of the two DSSCs fabricated without PANI and with 1.5 wt% PANI in the gel polymer electrolyte

Electrolyte	R_S (Ω)	$R1_{CT}$ (Ω)	$R2_{CT}$ (Ω)	$R3_{CT}$ (Ω)	f_{max} (Hz)	τ (ms)
0.0% PANI	17.60	11.20	14.10	11.70	15.69	10.14
1.5% PANI	14.20	3.01	9.60	3.08	20.84	7.63

have higher diffusion kinetics in the electrolyte. The lower value of $R3_{CT}$ correlates with the higher ionic conductivity of the electrolyte and higher J_{sc} of the solar cell made with 1.5% wt% PANI.

The lower $R2_{CT}$ value in the PANI-added DSSC system implies that the electron transfer mechanism at the TiO_2/electrolyte interface has also improved due to the presence of PANI in the electrolyte. This could be very likely due to the electronic conductivity nature of PANI. Moreover, the charge transfer resistance ($R1_{CT}$) at the Pt counter electrode of the DSSC made with PANI-added gel electrolyte is much lower than that of the DSSC made with normal electrolyte without PANI. This increase in the charge transfer ability at the Pt/electrolyte interface could also be due to the electronic conductivity nature of PANI. The fast transport of electrons from Pt counter electrode to the electrolyte is expected to accelerate the catalytic reduction reaction of iodides at this interface.

The bode phase plots of EIS spectra, as shown in Fig. 3, display the frequency peaks of the charge transfer process of two DSSCs with and without PANI. The electron lifetime (τ) in the DSSC can be determined from the value of the maximum frequency (f_{max}). Table 2 shows resistance values and electron lifetime values for the two DSSC systems fabricated with and without PANI in the electrolyte. From Table 2, it can be seen that the electron lifetime is lower for the cell with PANI in the electrolyte, which is consistent with the lower

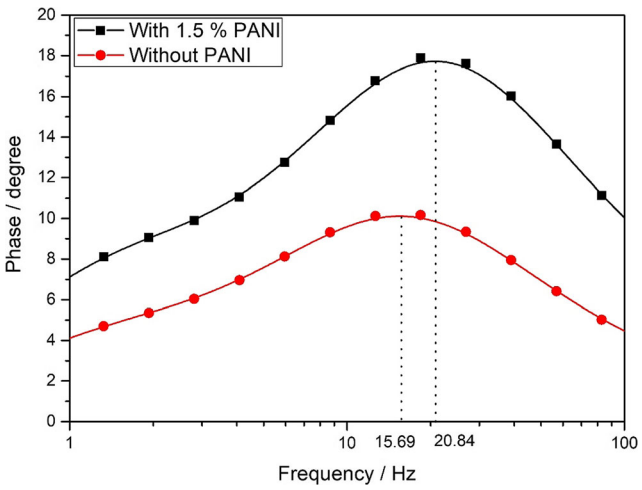

Fig. 3 Bode phase plots for the two DSSCs fabricated without PANI and with 1.5 wt% PANI in the gel polymer electrolyte

charge transfer resistance ($R2_{CT}$ = 9.60 Ω) value at the photoanode/electrolyte interface very likely due to the electronic conductivity of PANI [18, 22, 23].

Surface morphology analysis

Figure 4a shows the photograph of the gel electrolytes prepared with different amounts of PANI in inverted sample bottles to show the non-flowing gel nature of the electrolytes. Figure 4b and c show the SEM images of the electrolytes without PANI and with 1.5 wt% PANI respectively. SEM images show that the PANI-added electrolyte has more non-uniform and irregular surface consisting of more voids compared to the electrolyte without PANI. These two SEM images were analyzed by image analysis software (ImageJ) to estimate the surface porosity. The estimated porosity value for the electrolyte with 1.5 wt% PANI is 15.1% and the porosity value for the electrolyte without PANI is 3.7%. The increase in the porosity is an added advantage for the performance of the DSSC since the micro-porous structure is capable of trapping a large amount of liquid electrolyte in the pores while still retaining the quasi-solid or "gel" structure. Owing to the nature of interconnected porous framework, PANI molecular chains can also be easily diffused into the PEO matrix and interact effectively [20] with the proposed ionic transport process.

As a further experimental evidence for the plasticizing effect of the salt LiI and PANI, we give the optical microscopic images of the PEO electrolyte without and with PANI. Figure 5a and b show the polarized optical microscopic photographs of gel polymer electrolytes with only PEO and PEO/LiI/PANI, respectively. Figure 5a shows the crystalline nature of the spherulitic texture of PEO. According to Fig. 5b, when adding the LiI salt and PANI polymer, the size of the spherulites has been reduced and the dark areas representing the amorphous phase of PEO have also increased compared to those of Fig. 5a.

FTIR analysis

FTIR spectroscopy was used to study the interactions between PEO, LiI salt, and PANI conducting polymer. Figure 6a shows the FTIR spectrum of pure PEO, Fig. 6b shows the FTIR spectrum of PEO/LiI gel polymer electrolyte, and Fig.

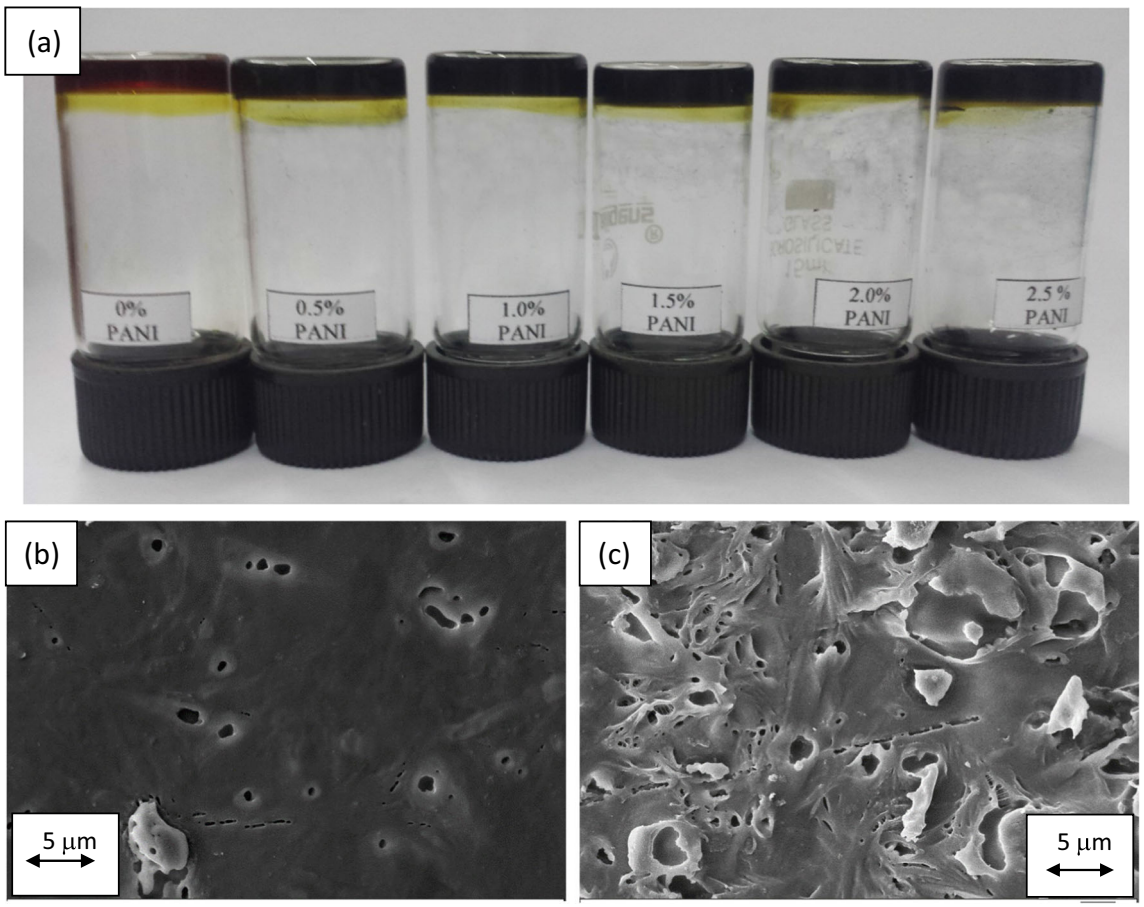

Fig. 4 **a** Photograph of samples of gel electrolytes in inverted bottles showing the non-flowing gel nature of the electrolyte. SEM images of surface of electrolyte without PANI (**b**) and with 1.5 wt% PANI (**c**)

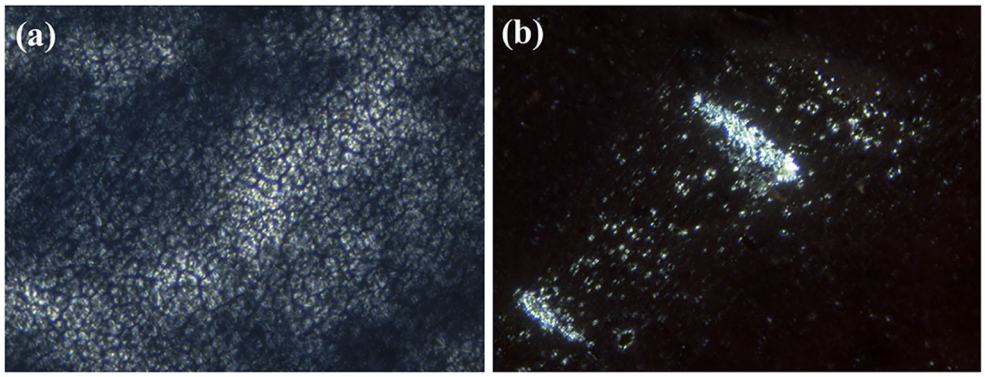

Fig. 5 Polarized optical microscopic photographs of the gel polymer electrolyte **a** with only PEO and **b** with PEO/LiI/PANI, respectively. In **a**, bright particles show the crystalline spherulites of pure PEO embedded in the amorphous phase (dark regions). In **b**, the reduced PEO crystalline spherulites and the dark background correspond to the increased amorphous nature of the electrolyte due to the addition of the salt (LiI) and PANI

6c shows the FTIR spectrum of PEO/LiI/1.5 wt% PANI gel electrolyte. For the two gel electrolytes, characteristic acetonitrile peaks can be observed at the wave number 2252 cm^{-1} for C-N stretching, at 1038 cm^{-1} for CH_3 rock, and at 920 cm^{-1} for C-C stretching. In the case of pure PEO, the C-O-C stretching mode is divided into three separate peaks at 1149, 1103, and 1061 cm^{-1} which confirms the presence of crystalline PEO in the PEO polymer [24, 25].

In our present work for pure PEO, CH_2 wagging mode can be observed at 843 cm^{-1}, CH_2 twisting mode at 963 cm^{-1}, and CH_2 bending vibrations at 1344 cm^{-1} and 1360 cm^{-1}, which indicates the crystallinity of PEO. Asymmetric CH_2 bending peak can be observed at 1467 cm^{-1}. These results are consistent with results reported by other workers [24–27]. The peak centered at 2890 cm^{-1} representing CH_2 stretching mode gets broadened with the addition of salt and broadened further with the addition of PANI, indicating a reduction of PEO crystallinity and an increase of its amorphous phase content [28] favoring ionic mobility.

With the introduction of the LiI salt and PANI, all the above peaks are shifted towards lower wave number side in the polymer-salt-PANI complex [29]. Most of the peaks are broadened after the addition of the salt and PANI, indicating a reduction of PEO crystallinity. With the incorporation of Li salt and PANI into the PEO matrix, the C-O-C triplet of PEO has combined to form a major peak at 1103 cm^{-1} which is slightly shifted to the lower wave number at 1097 cm^{-1} after adding LiI salt and 1096 cm^{-1} after adding 1.5 wt% PANI, respectively. Peaks at 1149 cm^{-1} and 1061 cm^{-1} have disappeared [30]. Table 3 summarizes the positions of important FTIR peaks and their possible assignments.

The sharp peaks at 1360 and 1344 cm^{-1} in PEO associated with crystalline nature have broadened after the addition of LiI salt and further broadened due to the addition of PANI, indicating reduced crystallinity and increased amorphous nature due to PANI. Similar observations can be made with the peak at 1467 cm^{-1} which, in addition to slight shifting in wavenumber, has also got broadened due to salt addition and further broadening due to PANI addition.

In the FTIR spectrum of the poly(ethylene oxide)-lithium difluoro(oxalato) borate (PEO-LiDFOB) solid polymer electrolyte system, Polu et al. have reported that CH_2 twisting mode at 963 cm^{-1} and CH_2 bending vibrations at 1343 and 1360 cm^{-1} which indicates the crystallinity of PEO have broadened due to the addition of the salt [29]. In the FTIR spectra of the PEO and PEO:LiTf polymer electrolyte system, Dissanayake et al. have observed that the strong bands at 1343, 1150, and 1113 cm^{-1} which are assigned to the crystalline phase have shoulders at 1350, 1142, and 1110 cm^{-1}, respectively, giving rise to broad bands at these frequencies due to the increase in the amorphous phase content due to thermal effect when the electrolyte temperature is raised from room temperature to 60 °C. The intensity of the doublet at 1360 and 1343 cm^{-1} has decreased with decreasing crystallinity [25].

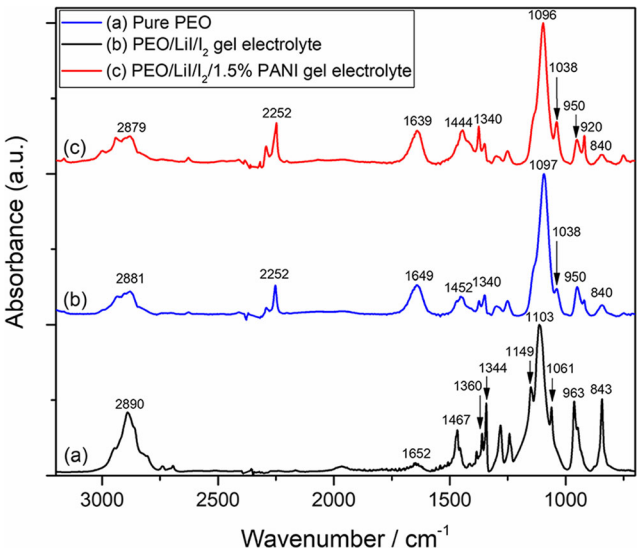

Fig. 6 FTIR spectra of pure PEO, PEO/LiI/I_2 gel electrolyte, and PEO/LiI/I_2/1.5 wt% PANI gel electrolyte

Table 3 Comparison of FTIR peaks (in cm^{-1}) in PEO, PEO/LiI, and PEO/LiI/1.5 wt% PANI systems

PEO	PEO:LiI	PEO:LiI:PANI
2890 CH_2 stretching	Peak shifted to 2881 and broadened evidently due to the PEO:Salt interaction.	Peak shifted to 2879 due to PEO-Li^+-PANI interaction causing cation immobilization facilitating salt dissociation at low salt concentrations.
1652 C=O stretching	Shifted to 1649, strong broad and intense peak due to salt-polymer interaction.	Shifted to lower energy at 1639 due to PANI-salt interaction.
1467 asymmetric CH_2 bending	Shifted to 1452 due to salt-PEO polymer interaction	Shifted to 1444 (to lower energy) and broadened due to PANI-salt interaction.
1344,1360 symmetric CH_2 bending	Shifted slightly to lower energy and broadened due to salt-polymer interaction (plasticizing effect)	1340 and 1360 peaks further broadened due to PANI
1103 C-O-C stretching	Shifted to 1097 lower energy; PEO polymer-salt interaction	Shifted slightly to 1096 lower energy; PANI-salt interaction.
963 asymmetric CH_2 rocking	950 lower energy; PEO polymer-salt interaction	950 no further shift
843 C-O stretching	840 lower energy; PEO polymer-salt interaction	840 no further shift

The effect of changes in the FTIR spectra in the1380–1330 cm^{-1} spectral region due to the addition of the plasticizer propylene carbonate (PC) on pure PEO has been studied by Frech and Chintapalli [31]. The peaks at 1360 and 1343 cm^{-1} associated with the crystalline phase of PEO have diminished in intensity due to the addition of PC, indicating the increase in the amorphous phase content. In the present study, due to the plasticizer effect of PANI, the two peaks at 1344 cm^{-1} and 1360 cm^{-1} have diminished in intensity and a new peak emerges at 1340 cm^{-1} quite similar to the effect of the plasticizer PC in the system reported by Frech and Chintapalli [31].

The shifts of FTIR absorption bands suggest that the PEO and PANI polymers both interact with the Li^+ ion in the salt. This appears to indicate that the Li^+ cations coordinate with oxygen atoms of PEO and nitrogen atoms of PANI polymer effectively "trapping" and immobilizing the Li^+ cations and thereby facilitating the ionic dissociation and releasing more free iodide (I^-) ions available for iodide ion conductivity. This substantiates the results obtained from the conductivity measurements which shows enhanced ionic conductivity due to the incorporation of 1.5 wt% PANI.

Ionic conductivity analysis

The ionic conductivity and activation energy, E_a, are key parameters used when studying the performance of electrolytes. The relationship between ionic conductivity at room temperature and the PANI content in the PEO-based composite polymer electrolytes is shown in Fig. 7. The maximum conductivity value of 1.87×10^{-3} S cm^{-1} at room temperature is obtained with the addition of 1.5 wt% PANI to the PEO/LiI electrolyte. The observed variation in conductivity can be explained by two competing effects: one is the increasing conductivity due to the decrease in the crystallinity and the corresponding increase in the amorphous phase content of the PEO-based polymer electrolyte due to the addition of the LiI salt and PANI coupled with the cation "trapping effect" and increasing ionic dissociation creating more iodide (I^-) ions mediated by PANI. The second is the "blocking effect" for ionic migration caused due to the presence of more PANI, which results in a decrease in conductivity. When more and more PANI beyond the maximum conductivity composition is added, the aggregation tendency of PANI particles reduces the available PANI sites for coordination and "trapping" Li^+ ions and obstructs the availability of more free I^- ions for ionic transport. This will reduce the overall conductivity of the electrolyte due to further addition of PANI [32].

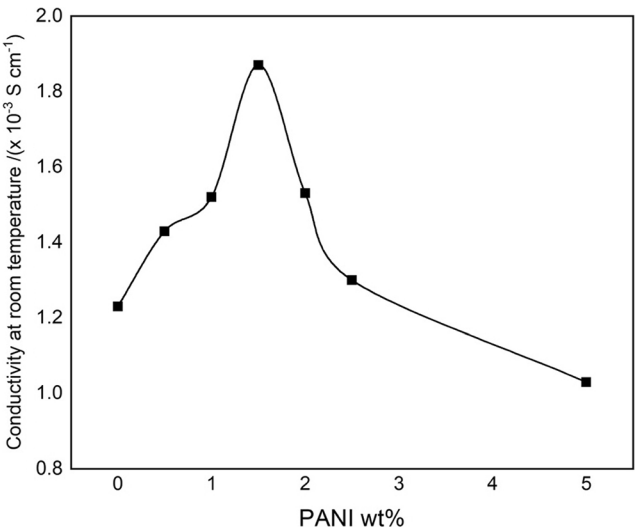

Fig. 7 Variation of conductivity of PEO/LiI/I_2/PANI at room temperature with the added amount of PANI

Plasticizers with relatively high dielectric constants such as ethylene carbonate (ε = 95) and propylene carbonate (ε = 65.5) are widely used to increase the ionic conductivity of polymer electrolytes by enhancing the dissociation of the ionic salt. The conducting polymer PANI (emeraldine salt) we have used as an additive to the PEO-based polymer electrolyte in this work has a high room temperature dielectric constant (ε) of 394. Therefore, one of the possibilities for the observed conductivity increase in the PANI-added electrolyte is the ability of PANI to act as a plasticizer, thereby increasing its amorphous phase content and enhancing the salt dissociation in the electrolyte and increasing the number of free I^- anions.

The ionic conductivity (σ) resulting from the transport of ionic species in an electrolyte medium is strongly dependent on the temperature. There are two forms of Arrhenius equations that are usually applied for explaining the ionic conductivity.

$$\sigma T = \sigma_o \exp(-E_a/k_B T) \tag{1}$$

and

$$\sigma' = \sigma'_o \exp(-E'_a/k_B T) \tag{2}$$

where T is the temperature, k_B is the Boltzmann constant, and E_a' and E_a'' are the activation energies for ion conduction for Eqs. (1) and (2), respectively. The pre-exponential terms σ_o and σ_o' of both equations are fundamentally different, including their units [33]. The σT (Eq. (1)), derived from Nernst–Einstein Eq. (3), expresses a direct relationship between the diffusion coefficient D of ionic migration and conductivity σ.

$$\sigma = \left(nq^2/kT\right)D \tag{3}$$

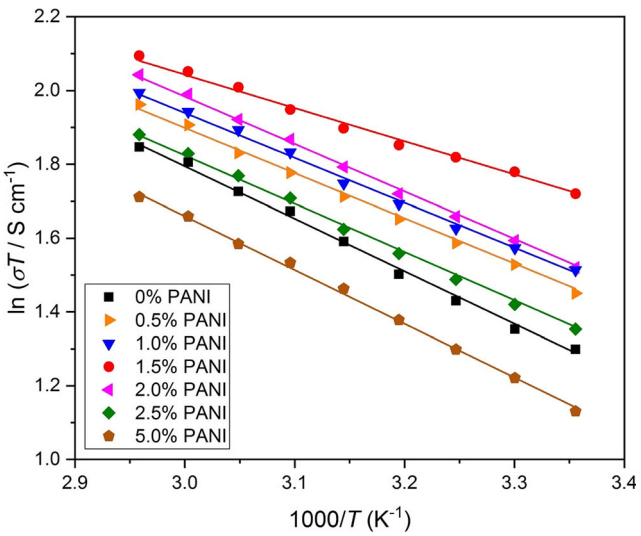

Fig. 8 Temperature dependence of ionic conductivity of the PEO/LiI/PANI polymer gel electrolytes with different amounts of added PANI

where n is the total concentration of the mobile ions. D is the carrier diffusion coefficient and k is Boltzmann's constant. In DSSC electrolytes based on iodide/tri-iodide redox mediator (I^-/I_3^-), iodide-tri-iodide ions migrate through the electrolyte medium driven by the concentration gradient of I^-/I_3^- anions. Therefore, in the present work, it is more accurate to interpret the conductivity data using the diffusion-mediated ionic migration-based σT (Eq. (1)). It should be mentioned here that another important empirical model generally used to study the ion transport in polymer electrolytes is the Vogel–Tammann–Fulcher (VTF) model based on Eq. (4).

$$\sigma(T) = AT^{-1/2}\exp[-B/k_B(T-T_o)] \tag{4}$$

In this model, a strong inter-relation between the conductivity and polymer segmental relaxation is anticipated. Cationic conductivity in PEO-based solid polymer electrolytes is best described by the VTF equation as there is a strong inter-relation between the cation migration and polymer segmental relaxation, implying that the polymer segmental relaxation and ionic motion are well coupled with each other [34, 35]. However, in the present study, we are dealing with anionic motion by diffusion in the electrolyte medium driven by concentration gradient of iodide ions. Therefore, the most appropriate equation is the σT Arrhenius (Eq. (1) given above).

A plot of ln σT vs 1/T gives a straight line for each electrolyte composition as shown in Fig. 8. As already discussed, the gradient of the linear part gives the activation energy for ionic motion and the lowest value is obtained for the 1.5 wt% PANI-added electrolyte. This is evidently related to the increased mobility of ions due to the increased amorphous nature of the PEO electrolyte due to the presence of PANI. Activation energy values are tabulated in Table 4.

Another important result can be obtained from linear fits (shown by dotted lines) to the series of straight lines in Fig. 8. The point of intersection of each extrapolated straight line with the y-axis at $x = 0$ is related to pre-exponential factor, σ_o in the above equation, which is proportional to the number

Table 4 Room temperature conductivity (σ) and activation energy of the PEO/LiI/PANI polymer gel electrolyte with different amounts of PANI

Added PANI wt%	σ at room temperature ($\times 10^{-3}$ S cm^{-1})	E_a (kJ mol^{-1})
0.0	1.23	11.99
0.5	1.43	10.19
1.0	1.52	10.12
1.5	1.87	7.49
2.0	1.53	10.69
2.5	1.30	10.87
5.0	1.03	12.10

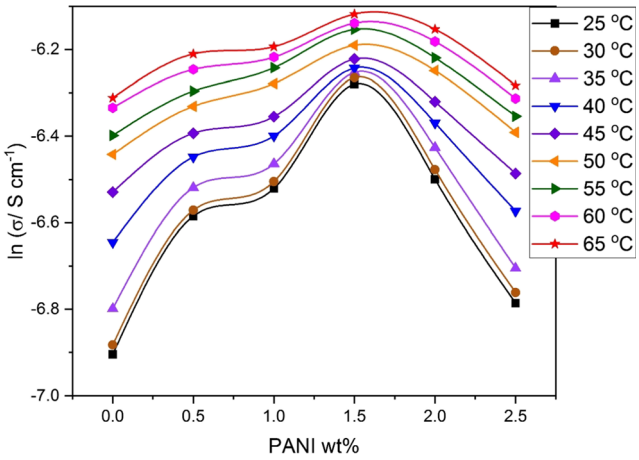

Fig. 9 Conductivity isotherms of the PEO/LiI/PANI polymer gel electrolytes with different amounts of added PANI. The curve for 5.0 wt% PANI composition has not been included to avoid overcrowding of curves

of mobile ions in the electrolyte. In the present case, these are predominantly the iodide ions (I^-) which are the mobile species contributing to the short circuit photocurrent in the DSSCs. It can be seen from Fig. 8 that the straight line which corresponds to the 1.5 wt% PANI-added electrolyte, when extrapolated, would intersect the *y*-axis at the highest point compared to the extrapolated straight lines of other samples. This agrees well with our suggestion that addition of 1.5 wt% PANI generates the highest number of mobile iodide ions evidently by ionic dissociation of LiI, compared to other PANI-added compositions. FTIR results confirm the coordination of PEO and PANI with Li^+ cations through Lewis acid base–type H-bonds effectively "*trapping*" and immobilizing the Li^+ ions, facilitating ionic dissociation and increasing the concentration of iodide ions (I^-) in the electrolyte medium. The increase in iodide ion conductivity in the electrolyte is determined by both the concentration of mobile iodide ions (n) and their mobility (μ). Both of these would contribute to an increase in iodide ion conductivity (σ) according to $\sigma = n\mu v_d$, where v_d is the diffusion mediated, effective drift velocity of iodide ions in the electrolyte medium. While PANI contributes to enhanced ionic mobility (μ) by decreasing the crystallinity of PEO as evident from the FTIR results, PANI also contributes to increase the number of mobile iodide ions (n) as seen from extrapolated straight lines in the ln (σT) vs 1/T plots (not shown).

We have made conductivity measurements on gel electrolyte samples containing the minimum amount of anhydrous acetonitrile and under dry, moisture free environment.

The lowest value of the activation energy (E_a) of 7.49 kJ mol^{-1} is exhibited by the electrolyte containing 1.5 wt% PANI. As seen from the FTIR results, this electrolyte composition has the lowest crystallinity and the highest amorphous phase content and therefore can be expected to have the lowest activation energy and therefore highest ionic mobility for I^- and I_3^- ion migration. Therefore, this electrolyte composition is expected to significantly enhance the charge transport kinetics of the corresponding DSSCs. The conductivity isotherms depicted in Fig. 9 clearly show that the electrolyte composition with 1.5 wt% PANI gives the highest conductivity at all measured temperatures and that compositions with higher PANI content have lower conductivity values.

Effect of iodide ion transport on DSSC efficiency

The effect of PANI-mediated iodide ion conductivity enhancement and enhanced DSSC efficiency can now be interpreted clearly using the schematic diagram shown in Fig. 10. It is clear that the addition of 1.5 wt% PANI to the PEO polymer gel electrolyte has enhanced the J_{sc} and the

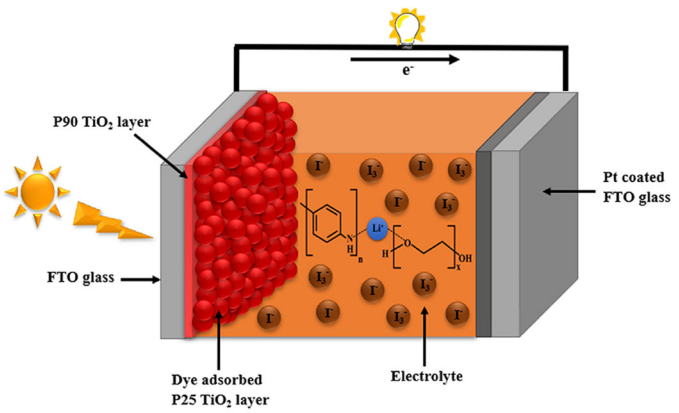

Fig. 10 Schematic diagram depicting PANI-mediated Li^+ ion trapping by coordination with oxygen in PEO and nitrogen in PANI facilitating ionic dissociation, releasing more free iodide (I^-) ions contributing to enhanced short circuit photocurrent and DSSC efficiency

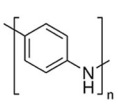

= This symbol in the Figure represents the Polyaniline (emeraldine salt).

overall solar cell efficiency evidently due to the increased iodide ion conductivity caused by the reduced crystallinity of the PEO-salt complex due to the plasticizing effect of PANI as well as the increased ionic dissociation due to the *cation trapping effect* of PANI. The presence of more amorphous regions in the PANI-incorporated electrolyte also improves the contact interface area between the TiO_2 photoanode and the electrolyte of the DSSC, thereby contributing to the increase in the short circuit photocurrent, J_{sc}. Figure 10 depicts a schematic diagram of the DSSC showing the "cation trapping effect" by salt-PANI and salt-PEO interactions in the polymer electrolyte medium allowing more iodide ions to be available for iodide ion conductivity.

Conclusions

Gel polymer electrolytes consisting of PEO/LiI/I_2 and incorporating different amounts of PANI were fabricated. The gel polymer electrolyte without PANI showed a conductivity of 1.23×10^{-3} S cm^{-1} at room temperature and with the incorporation of 1.5 wt% PANI, the conductivity increased up to 1.87×10^{-3} S cm^{-1}. FTIR studies confirmed that the coordination of PEO and PANI with Li^+ cations through Lewis acid base–type H-bonds effectively "traps" or immobilizes the Li^+ ions, facilitating ionic dissociation and increasing the number of iodide ions (I^-) in the electrolyte medium. The temperature dependence of ionic conductivity of these polymer electrolytes obeyed the Arrhenius relationship and the lowest activation energy of 7.49 kJ mol^{-1} is obtained for 1.5 wt% PANI-added composition. According to the FTIR results, the addition of PANI appears to decrease the crystallinity and increase the amorphous content of the PEO-based electrolyte. These effects due to the addition of PANI have increased the short circuit current density and the energy conversion efficiency of the DSSCs made with this optimized redox electrolyte. SEM analysis revealed that the addition of PANI improves the porosity of the electrolyte providing more pores within the polymer network to increase the amount of liquid electrolyte trapped in these polymer cages. The highest power conversion efficiency of 6.56% was obtained for the DSSC made using the polymer gel electrolyte with optimized PANI composition. This is an impressive 31% increase in efficiency in comparison with 5.00% for the DSSC made with a similar electrolyte without PANI.

Funding Funds were provided by the National Science Foundation of Sri Lanka under Grant No. NSF-PSF/ICRP/2017/EA&ICT/04.

Compliance with ethical standards

Conflict of interest The authors declare that they have no conflict of interest.

References

1. O'Regan B, Grätzel M (1991) A low-cost, high-efficiency solar cell based on dye-sensitized colloidal TiO_2 films. Nature 353:737–740
2. Yang H, Huang M, Wu J, Lan Z, Hao S (2008) The polymer gel electrolyte based on poly(methyl methacrylate) and its application in quasi-solid-state dye-sensitized solar cells. Matter Chem Phys 110:38–42
3. Law CH, Pathirana SC, Li X, Anderson AY, Barnes PRF, Listorti A, Ghaddar TH, O'Regan B (2010) Water-based electrolytes for dye-sensitized solar cells. Adv Mater 22:4505–4509
4. Bella F, Gerbaldi C, Barolo C, Grätzel M (2015) Aqueous dye-sensitized solar cells. Chem Soc Rev 44:3431–3473
5. Bella F, Galliano S, Piana G, Giacona G, Viscardi G, Grätzel M, Barolo C, Gerbaldi C (2019) Boosting the efficiency of aqueous solar cells: a photoelectrochemical estimation on the effectiveness of $TiCl_4$ treatment. Electrochim Acta 302:31–37
6. Galliano S, Bella F, Piana G, Giacona G, Viscardi G, Gerbaldi C, Grätzel M, Barolo C (2018) Finely tuning electrolytes and photoanodes in aqueous solar cells by experimental design. Sol Energy 163:251–255
7. Glinka A, Gierszewski M, Ziółek M (2018) Effects of aqueous electrolyte, active layer thickness and bias irradiation on charge transfer rates in solar cells sensitized with top efficient carbazole dyes. J Phys Chem C 122:8147–8158
8. Lin RY-Y, Wu F-L, Li C-T, Chen P-Y, Ho K-C, Lin JT (2015) High-performance aqueous/organic dye-sensitized solar cells based on sensitizers containing triethylene oxide methyl ether. Chem Sus Chem 8:2503–2513
9. Zhong Y, Xia X, Mai W, Tu J, Fan HJ (2017) Integration of energy harvesting and electrochemical storage devices. Adv Mater Technol 2(12):1700182
10. Scalia A, Varzi A, Lamberti A, Jacob T, Passerini S (2018) Portable high voltage integrated harvesting-storage device employing dye-sensitized solar module and all-solid-state electrochemical double layer capacitor. Front Chem 6:00443
11. Selvaraj P, Baig H, Mallick TK, Siviter J, Montecucco A, Li W, Paul M, Sweet T, Gao M, Knox AR, Sundarama S (2018) Enhancing the efficiency of transparent dye-sensitized solar cells using concentrated light. Sol Energy Mater Sol Cells 175:29–34
12. Cannavale A, Martellotta F, Fiorito F, Ayr U (2020) The challenge for building integration of highly transparent photovoltaics and photoelectrochromic devices. Energies 13:1929. https://doi.org/10.3390/en13081929
13. Wu J, Hao S, Lan Z, Lin J, Huang M, Huang Y, Li P, Yin S, Sato T (2008) An all-solid-state dye-sensitized solar cell based poly(N-alkyl-4-vinyl-pyridine iodide) electrolyte with efficiency of 5.64%. J Am Chem Soc 130:11568–11569
14. Li Q, Chen X, Tang Q, Xu H, He B, Qin Y (2013) Imbibition of polypyrrole into three-dimensional poly(hydroxyethyl methacrylate/glycerol) gel electrolyte for robust quasi-solid-state dye-sensitized solar cells. J Mater Chem 1:8055–8060
15. Reddy MJ, Chu PP (2002) Optical microscopy and conductivity of poly(ethylene oxide) complexed with KI salt. Electrochim Acta 47:1189–1196
16. Dissanayake MAKL, Ekanayake EMBS, Bandara LRAK, Seneviratne VA, Thotawatthage CA, Jayaratne SL, Senadeera GKR (2016) Efficiency enhancement by mixed cation effect in poly ethylene oxide (PEO)-based dye-sensitized solar cells. J Solid State Electrochem 20:193–201
17. Yuan S, Tang Q, He B, Yu L (2015) Conducting gel electrolytes with microporous structures for efficient quasi-solid-state dye-sensitized solar cells. J Power Sources 273:1148–1155
18. Duan Y, Tang Q, Chen Y, Zhao Z, Lv Y, Hou M, Yang P, He B, Yu L (2015) Solid-state dye-sensitized solar cells from poly(ethylene

oxide)/polyaniline electrolytes with catalytic and hole-transporting characteristics. J Mater Chem A 3:5368–5374
19. Yang Y, Zhang J, Zhou CH, Wu SJ, Liu W, Han HW, Chen BI, Zhao X-Z (2008) Effect of Lithium iodide addition on poly(ethylene oxide)-poly(vinylidene fluoride) polymer blend electrolyte for dye-sensitized nanocrystalline solar cell. J Phys Chem B 112:6594–6602
20. Liow KS, Sipaut CS, Jafarzadeh M (2018) Polypyrrole and polyaniline surface modified nanosilica as quasi-solid-state electrolyte ingredients for dye-sensitized solar cells. J Mater Sci Mater Electron 29:21097–21108
21. Dissanayae MAKL, Kumari JMKW, Senadeera GKR, Thotawatthage CA, Mellander B-E, Albinsson I (2017) A novel multilayered photoelectrode with nitrogen doped TiO_2 for efficiency enhancement in dye sensitized solar cells. J Photochem Photobiol A 349:63–72
22. Kumari JMKW, Senadeera GKR, Dissanayake MAKL, Thotawatthage CA (2017) Dependence of photovoltaic parameters on the size of cations adsorbed by TiO_2 photoanode in dye-sensitized solar cells. Ionics 23:2895–2900
23. Dissanayae MAKL, Kumari JMKW, Senadeera GKR, Thotawatthage CA (2016) Efficiency enhancement in plasmonic dye-sensitized solar cells with TiO_2 photoanodes incorporating gold and silver nanoparticles. J Appl Electrochem 46:47–58
24. Tang Z, Wang J, Chena Q, He Q, Shen C, Mao XX, Zhang J (2007) A novel PEO-based composite polymer electrolyte with absorptive glass mat for Li-ion batteries. Electrochem Acta 52:6638–6643
25. Dissanayake MAKL, Frech R (1995) Infrared spectroscopic study of the phases and phase transitions in poly(ethylene oxide) and poly(ethylene oxide)-lithium trifluoromethanesulfonate complexes. Macromolecules 28(15):5312–5319
26. Rajendran S, Kannan R, Mahendran O (2001) Ionic conductivity studies in poly(methyl methacrylate)-polyethylene oxide hybrid polymer electrolytes with lithium salts. J Power Sources 96:406–410
27. Ramesh S, Yuen TF, Shen CJ (2008) Conductivity and FTIR studies on PEO-LiX [X: $CF_3SO_3^-$, SO_4^{2-}] polymer electrolytes. Spectrochim Acta 69:670–675
28. Sundar M, Selladurai S (2006) Effect of fillers on magnesium-poly(ethylene oxide) solid polymer electrolyte. Ionics 12:281–286
29. Polu AR, Kim DK, Rhee H-W (2015) Poly(ethylene oxide)-lithium difluoro(oxalato)borate new solid polymer electrolytes: ion-polymer interaction, structural, thermal, and ionic conductivity studies. Ionics 21:2771–2780
30. Rocco AM, Bielschowsky CE, Pereira R (2003) Blends of poly(-ethylene oxide) and poly(4-vinylphenol-co-2-hydroxyethyl methacrylate): thermal analysis, morphological behaviour and specific interactions. Polymer 44:361–368
31. Frech R, Chintapalli S (1996) Effect of propylene carbonate as a plasticizer in high molecular weight PEO-$LiCF_3SO_3$ electrolytes. Solid State Ionics 85:61–66
32. Capiglia C, Mustarelli P, Quartarone E, Tomasi C, Magistris CA (1999) Effects of nanoscale SiO_2 on the thermal and transport properties of solvent-free, poly(ethylene oxide) (PEO)-based polymer electrolytes. Solid State Ionics 118:73–79
33. Nuernberg RB (2020) Numerical comparison of usual Arrhenius-type equations for modelling ionic transport in solids. Ionics 26: 2405–2412
34. Aziz Shujahadeen B, Woo Thompson J, Kadir MFZ, Ahmed Hameed M (2018) A conceptual review on polymer electrolytes and ion transport models. J Sci Adv Mater Dev 3(1):1–17
35. Pitawala HMJC, Dissanayake MAKL, Seneviratne VA, Mellander B-E, Albinson I (2008) Effect of plasticizers (EC or PC) on the ionic conductivity and thermal properties of the $(PEO)_9LiTf$: Al_2O_3 nanocomposite polymer electrolyte system. J Solid State Electrochem 12:783–789